GAUSSIAN RANDOM PARTICLES WITH FLEXIBLE HAUSDORFF DIMENSION

LINDA V. HANSEN,* *Varde College*

THORDIS L. THORARINSDOTTIR,** *Norwegian Computing Center*

EVGENI OVCHAROV,*** **** *Heidelberg Institute for Theoretical Studies*

TILMANN GNEITING,*** ***** *Heidelberg Institute for Theoretical Studies*
and Karlsruhe Institute of Technology

DONALD RICHARDS,****** *Penn State University*

Abstract

Gaussian particles provide a flexible framework for modelling and simulating three-dimensional star-shaped random sets. In our framework, the radial function of the particle arises from a kernel smoothing, and is associated with an isotropic random field on the sphere. If the kernel is a von Mises–Fisher density, or uniform on a spherical cap, the correlation function of the associated random field admits a closed form expression. The Hausdorff dimension of the surface of the Gaussian particle reflects the decay of the correlation function at the origin, as quantified by the fractal index. Under power kernels we obtain particles with boundaries of any Hausdorff dimension between 2 and 3.

Keywords: Celestial body; correlation function; fractal dimension; Lévy basis; random field on a sphere; simulation of star-shaped random set

2010 Mathematics Subject Classification: Primary 60D05
Secondary 60G60; 37F35

1. Introduction

Mathematical models for three-dimensional particles have received great interest in astronomy, botany, geology, material science, and zoology, among many other disciplines. While some particles such as crystals have a rigid shape, many real-world objects are star-shaped, highly structured, and stochastically varying (Wicksell (1925), Stoyan and Stoyan (1994)). As a result, flexible yet parsimonious models for star-shaped random sets have been in high demand. Grenander and Miller (1994) proposed a model for two-dimensional featureless objects with no obvious landmarks, which are represented by a deformed polygon along with a Gaussian shape model. This was investigated further by Kent *et al.* (2000) and Hobolth *et al.* (2002), and a non-Gaussian extension was suggested by Hobolth *et al.* (2003). Miller *et al.* (1994) proposed an isotropic deformation model that relies on spherical harmonics and was studied

by Hobolth *et al.* (2003), where it was applied to monitor tumour growth. A related Gaussian random shape model was studied by Muinonen *et al.* (1996) and used by Muñoz *et al.* (2007) to represent Saharan desert dust particles.

In this paper we propose a flexible framework for modelling three-dimensional star-shaped particles, where the radial function is a random field on the sphere that arises through a kernel smoothing. Specifically, let $Y \subset \mathbb{R}^3$ be a three-dimensional compact set, which is star-shaped with respect to an interior point o. Then there is a one-to-one correspondence between the set Y and its radial function $X = \{X(u) : u \in \mathbb{S}^2\}$, where

$$X(u) = \max\{r \geq 0 : o + ru \in Y\}, \qquad u \in \mathbb{S}^2,$$

with $\mathbb{S}^2 = \{x \in \mathbb{R}^3 : \|x\| = 1\}$ denoting the unit sphere in $\mathbb{R}^3$. We model X as a real-valued random field on $\mathbb{S}^2$ via a kernel smoothing of a Gaussian measure, in that

$$X(u) = \int_{\mathbb{S}^2} K(v, u) L(\mathrm{d}v), \qquad u \in \mathbb{S}^2, \tag{1}$$

where $K : \mathbb{S}^2 \times \mathbb{S}^2 \to \bar{\mathbb{R}}$ is a suitable kernel function, and L is a Gaussian measure on the Borel subsets of $\mathbb{S}^2$. That is, $L(A) \sim \mathcal{N}(\mu\lambda(A), \sigma^2\lambda(A))$ with parameters $\mu \in \mathbb{R}$ and $\sigma^2 > 0$, where $\lambda(A)$ denotes the surface measure of a Borel set $A \subseteq \mathbb{S}^2$, with $\lambda(\mathbb{S}^2) = 4\pi$.

If X were a nonnegative process, the random particle could be described as the set

$$Y = \bigcup_{u \in \mathbb{S}^2} \{o + ru : 0 \leq r \leq X(u)\} \subset \mathbb{R}^3,$$

so that the particle contains the centre o, which without loss of generality can be assumed to be the origin, and the distance in direction u from o to the particle boundary is given by $X(u)$. A potentially modified particle Y_c arises in the case of a general, not necessarily nonnegative process, where we replace $X(u)$ by $X_c(u) = \max(c, X(u))$ for some $c > 0$. We call Y or Y_c a Gaussian particle, with realisations being illustrated in Figure 1. The Gaussian particle framework is a special case of the linear spatio-temporal Lévy model proposed by Jónsdóttir *et al.* (2008) in the context of tumour growth. Alternatively, it can be seen as a generalisation and a three-dimensional extension of the model proposed by Hobolth *et al.* (2003), while also being a generalisation of the Gaussian random shape models of Miller *et al.* (1994) and Muinonen *et al.* (1996).
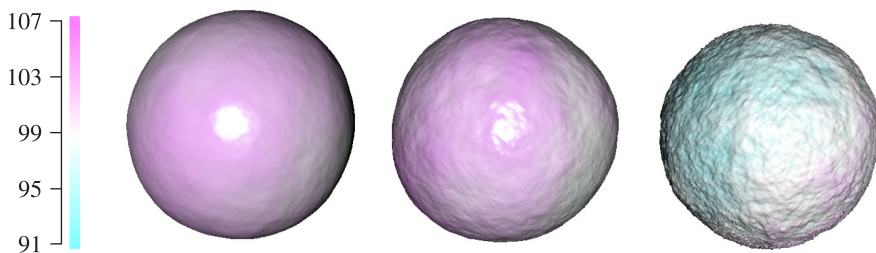

FIGURE 1: Gaussian particles with mean $\mu_X = 100$ and variance $\sigma_X^2 = 10$, using the power kernel (8) with $q = 0.05$ (left), $q = 0.25$ (middle), and $q = 0.5$ (right). The Hausdorff dimension of the particle surface equals $2 + q$.

The realisations in Figure 1 demonstrate that the boundary or surface of a Gaussian particle allows for regular as well as irregular behaviour. The roughness or smoothness of the surface in the limit as the observational scale becomes infinitesimally fine can be quantified by the Hausdorff dimension, which for a surface in $\mathbb{R}^3$ varies between 2 and 3, with the lower limit corresponding to a smooth, differentiable surface, and the upper limit corresponding to an excessively rough, space-filling surface (Falconer (1990)). The Hausdorff dimension of the surface of an isotropic Gaussian particle is determined solely by the behaviour of the correlation function of the associated random field on the sphere. We investigate the properties of Gaussian particles under parametric families of isotropic kernel functions, including power kernels, and kernels that are proportional to von Mises–Fisher densities (Fisher *et al.* (1987)), or uniform on spherical caps. Under power kernels we obtain particles with boundaries of any Hausdorff dimension between 2 and 3. Von Mises–Fisher and uniform kernels generate Gaussian particles with boundaries of Hausdorff dimension 2 and 2.5, respectively.

The remainder of the paper is organised as follows. In Section 2 we recall the basic properties of the radial function in the Gaussian particle model (1). In Section 3 we show how to derive the Hausdorff dimension of an isotropic Gaussian particle from the infinitesimal behaviour of the correlation function of the underlying random field at the origin. In Section 4 we introduce the aforementioned families of isotropic kernels and discuss the properties of the associated correlation functions and Gaussian particles, with some technical arguments deferred to Appendix A. In Section 5 we present a simulation algorithm and simulation examples, including a case study on celestial bodies and a discussion of planar particles. The paper concludes with a discussion in Section 6.

2. Preliminaries

The properties of the random function (1) that characterises a Gaussian particle process depend on the kernel function K. We assume that K is isotropic, in that $K(v, u) = k(d(v, u))$ depends on the points $v, u \in \mathbb{S}^2$ through their great circle distance $d(v, u) \in [0, \pi]$ only. As $d(v, u) = \arccos(u \cdot v)$, this is equivalent to assuming that the kernel depends on the inner product $u \cdot v$ only. The results of Jónsdóttir *et al.* (2008) in concert with the rotation invariance property following from an isotropic kernel imply that the mean function $\mathbb{E}(X(u))$ and the variance function $\text{var}(X(u))$ are constant, that is,

$$\mu_X = \mathbb{E}(X(u)) = \mu c_1 \quad \text{and} \quad \sigma_X^2 = \text{var}(X(u)) = \sigma^2 c_2$$

for $u \in \mathbb{S}^2$, where we assume that

$$c_n = \int_{\mathbb{S}^2} k(d(v, u))^n \, dv$$

is finite for $n = 1, 2$.

Note that X is a stochastic process on the sphere (Jones (1963)), whose covariance function is given by

$$\text{cov}(X(u_1), X(u_2)) = \sigma^2 \int_{\mathbb{S}^2} k(d(v, u_1)) k(d(v, u_2)) \, dv, \qquad u_1, u_2 \in \mathbb{S}^2.$$

Under an isotropic kernel, the random field X is isotropic as well, and it is readily seen that

$\mathrm{cor}(X(u_1), X(u_2)) = C(d(u_1, u_2))$, where

$$C(\theta) = \frac{2}{c_2} \int_0^\pi \int_0^\pi k(\eta) k(\arccos(\sin\theta \sin\eta \cos\phi$$
$$+ \cos\theta \cos\eta)) \, \mathrm{d}\phi \sin\eta \, \mathrm{d}\eta, \qquad 0 \le \theta \le \pi, \qquad (2)$$

is the correlation function of the random field X. As recently shown by Ziegel (2014), any continuous isotropic correlation function on a sphere admits a representation of this form.

3. The Hausdorff dimension

The Hausdorff dimension of a set $Z \subset \mathbb{R}^d$ is defined as follows (Hausdorff (1918)). For $\varepsilon > 0$, an ε-cover of Z is a countable collection $\{B_i : i = 1, 2, \ldots\}$ of balls $B_i \subset \mathbb{R}^d$ of diameter $|B_i|$ less than or equal to ε that covers Z. With

$$H^\delta(Z) = \lim_{\varepsilon \to 0} \inf \left\{ \sum_{i=1}^\infty |B_i|^\delta : \{B_i : i = 1, 2, \ldots\} \text{ is an } \varepsilon\text{-cover of } Z \right\}$$

denoting the δ-dimensional Hausdorff measure of Z, there exists a unique nonnegative number δ_0 such that $H^\delta(Z) = \infty$ if $\delta < \delta_0$ and $H^\delta(Z) = 0$ if $\delta > \delta_0$. This number δ_0 is the Hausdorff dimension of the set Z. Note that we have defined the Hausdorff measure using coverings with balls. This approach is consistent with the treatments given by Adler (2010) and Hall and Roy (1994) and simplifies the presentation.

As X is a kernel smoothing of a Gaussian measure, X has Gaussian finite dimensional distributions and, thus, is a Gaussian process. While there are a wealth of results on the Hausdorff dimension of the graphs of stationary Gaussian random fields on Euclidean spaces, which is determined by the infinitesimal behaviour of the correlation function at the origin, as formalised by the fractal index (Hall and Roy (1994), Adler (2010)), we are unaware of any extant results for the graphs of random fields on spheres, or for the surfaces of star-shaped random particles.

We now state and prove such a result. Toward this end, we say that an isotropic random field X on the sphere with correlation function $C : [0, \pi] \to \mathbb{R}$ has fractal index $\alpha > 0$ if there exists a constant $b > 0$ such that

$$\lim_{\theta \downarrow 0} \frac{C(0) - C(\theta)}{\theta^\alpha} = b. \qquad (3)$$

The fractal index exists for essentially all correlation functions of practical interest, and it is always true that $\alpha \in (0, 2]$. To see this, suppose that $C : [0, \pi] \to \mathbb{R}$ is an isotropic correlation function on the two-dimensional sphere. Clearly, C is also an isotropic correlation function on the circle. Furthermore, its even, 2π-periodic continuation to $\mathbb{R}$ is a stationary correlation function on the real line. Therefore, the corresponding restriction on Euclidean spaces ((Adler (2010) p. 200)) applies, in that $\alpha \in (0, 2]$.

The following theorem relates the Hausdorff dimension of the graph of an isotropic Gaussian random field X on the sphere $\mathbb{S}^2$ to its fractal index. The proof employs stereographic projections that allow us to draw on classical results in the Euclidean case.

Theorem 1. *Let X be an isotropic Gaussian random field on $\mathbb{S}^2$ with fractal index $\alpha \in (0, 2]$. Consider the random surface*

$$Z_c = \{(u, X_c(u)) : u \in \mathbb{S}^2\},$$

where $X_c(u) = \max(c, X(u))$ with $c > 0$. Then with probability 1 either of the following alternatives hold.

(a) *If $\max_{u \in \mathbb{S}^2} X(u) \leq c$, the realisation of Z_c is the sphere with radius c and so its Hausdorff dimension is 2.*

(b) *If $\max_{u \in \mathbb{S}^2} X(u) > c$, the realisation of Z_c has Hausdorff dimension $3 - \alpha/2$.*

Proof. The claim in (a) is trivial. To prove the statement in (b), we assume without loss of generality that $X(u_0) > c$, where $u_0 = (0, 0, 1)$. The sample paths of X are continuous almost surely according to Gangolli ((1967) Theorem 7.2). Thus, there exists an $\varepsilon \in (0, \frac{1}{2})$ such that $X(u) > c$ for u in the spherical cap $\mathbb{S}^2_\varepsilon = \{u \in \mathbb{S}^2 : d(u, u_0) \leq \varepsilon\}$ of radius ε centred at u_0. Let $\Pi : \mathbb{S}^2_\varepsilon \to \mathbb{B}_\varepsilon$ define a stereographic projection that maps $(0, 0, 1)$ to $(0, 0)$, where $\mathbb{B}_\varepsilon = \{x = (x_1, x_2) \in \mathbb{R}^2 : x_1^2 + x_2^2 \leq \varepsilon^2\}$. A stereographic projection is a local diffeomorphism, Π, thus, is differentiable and has a differentiable inverse Π^{-1}, which is locally bi-Lipschitz (do Carmo (1976)). We may, therefore, assume that ε is small enough so that for all $x, x' \in \mathbb{B}_\varepsilon$ there exists a constant $A \geq 1$ with

$$\frac{1}{A}\|x - x'\| \leq \|\Pi^{-1}(x) - \Pi^{-1}(x')\| \leq A\|x - x'\|, \tag{4}$$

where $\|\cdot\|$ denotes the Euclidean norm on $\mathbb{R}^2$ or $\mathbb{R}^3$. Without loss of generality, we may in the following consider conditional probabilities which depend on the choice of u_0 and ε. Let the Gaussian random field W on $\mathbb{B}_\varepsilon \subset \mathbb{R}^2$ be given by $W(x) = X(\Pi^{-1}(x))$. From Xue and Xiao ((2011) Theorem 5.1), see also Adler ((2010) Chapter 8), the graph $\mathrm{Gr}\,W = \{(x, W(x)) : x \in \mathbb{B}_\varepsilon\}$ has Hausdorff dimension $3 - \alpha/2$ almost surely if there exists a constant $M_0 > 1$ such that

$$\frac{1}{M_0} \sum_{j=1}^{2} |x_j - x'_j|^\alpha \leq \mathbb{E}(W(x) - W(x'))^2 \leq M_0 \sum_{j=1}^{2} |x_j - x'_j|^\alpha \tag{5}$$

for all $x, x' \in \mathbb{B}_\varepsilon$. Letting $\vartheta(x, x') = d(\Pi^{-1}(x), \Pi^{-1}(x'))$, we have

$$\mathbb{E}(W(x) - W(x'))^2 = 2\sigma_X^2[C(0) - C(\vartheta(x, x'))], \tag{6}$$

where $C : [0, \pi] \to \mathbb{R}$ is the correlation function of the isotropic random field X. As chord length and great circle distance are bi-Lipschitz equivalent metrics, there exists a constant $B > 1$ such that

$$\frac{1}{B}\|\Pi^{-1}(x) - \Pi^{-1}(x')\| \leq \vartheta(x, x') \leq B\|\Pi^{-1}(x) - \Pi^{-1}(x')\|. \tag{7}$$

As the random field X is of fractal index α, there exists a constant $M_1 > 0$ such that

$$\sum_{j=1}^{2} |x_j - x'_j|^\alpha \leq 2^{1-\alpha/2}\|x - x'\|^\alpha \leq 2^{1-\alpha/2} A^\alpha B^\alpha \vartheta(x, x')^\alpha \leq M_1[C(0) - C(\vartheta(x, x'))]$$

for $x, x' \in \mathbb{B}_\varepsilon$ and $\varepsilon > 0$ sufficiently small, where the first estimate is justified by Jensen's inequality and the second by (4) and (7). Similarly, there exists a constant $M_2 > 0$ such that

$$M_2[C(0) - C(\vartheta(x, x'))] \leq \sum_{j=1}^{2} |x_j - x'_j|^\alpha$$

for all $x, x' \in \mathbb{B}_\varepsilon$ and $\varepsilon > 0$ sufficiently small. In view of (6), this proves the existence of a constant $M_0 > 1$ such that (5) holds, given that $\varepsilon > 0$ is sufficiently small.

Now, consider the mapping ζ from $\mathbb{B}_\varepsilon \times \mathbb{R}$ to $\mathbb{S}^2_\varepsilon \times \mathbb{R}$ defined by $\zeta(x, r) = (\Pi^{-1}(x), r)$, so that $\zeta(\mathrm{Gr} W) = \{(u, X(u)) : u \in \mathbb{S}^2_\varepsilon\}$. The identity

$$\|\zeta(x, r) - \zeta(x', r')\|^2 = \|\Pi^{-1}(x) - \Pi^{-1}(x')\|^2 + |r - r'|^2,$$

along with (4) implies ζ to be bi-Lipschitz. Therefore, by Proposition 3.3 of Falconer (1990), the partial surface $\{(u, X(u)) : u \in \mathbb{S}^2_\varepsilon\}$ has Hausdorff dimension $3 - \alpha/2$ almost surely. Invoking the countable stability property (Falconer (1990, p. 49)), we see that the full surface $Z_c = \{(u, X_c(u)) : u \in \mathbb{S}^2_\varepsilon\}$ also has Hausdorff dimension $3 - \alpha/2$ almost surely.

4. Isotropic kernels

It is often desirable that the surface of the particle process possesses the same Hausdorff dimension as that of the real-world particles to be emulated (Mandelbrot (1982), Orford and Whalley (1983), Turcotte (1987)). With this in mind, we introduce and study three one-parameter families of isotropic kernels for the Gaussian particle process (1). The families yield interesting correlation structures, and we study the asymptotic behaviour at 0, which determines the Hausdorff dimension of the Gaussian particle surface.

4.1. Von Mises–Fisher kernel

Here, we consider k to be the unnormalised von Mises–Fisher density,

$$k(\theta) = e^{a \cos \theta}, \qquad 0 \le \theta \le \pi,$$

with parameter $a > 0$. The von Mises–Fisher density with parameter $a > 0$ is widely used in the analysis of spherical data (Fisher *et al.* (1987)), and in this context a is called the precision. Straightforward calculations show that

$$C(\theta) = \frac{2}{\sinh(2a)} \frac{\sinh(a\sqrt{2(1 + \cos \theta)})}{\sqrt{2(1 + \cos \theta)}}, \qquad 0 \le \theta \le \pi,$$

from which it is readily seen that the fractal index is $\alpha = 2$. The surfaces of the corresponding Gaussian particles are smooth and have Hausdorff dimension 2, independently of the value of the parameter $a \in \mathbb{R}$.

4.2. Uniform kernel

We now let the kernel k be uniform, in that

$$k(\theta) = \mathbf{1}_{\{\theta \le r\}}, \qquad 0 \le \theta \le \pi,$$

with cut-off parameter $r \in (0, \pi/2]$, where $\mathbf{1}_{\{\cdot\}}$ denotes the indicator function. As shown in the appendix of Tovchigrechko and Vasker (2001), the associated correlation function is

$$C(\theta) = \frac{1}{\pi(1 - \cos r)} \left(\pi - \arccos\left(\frac{\cos \theta - \cos^2 r}{1 - \cos^2 r} \right) \right.$$
$$\left. - 2 \cos r \arccos\left(\cot r \frac{1 - \cos \theta}{\sin \theta} \right) \right) \mathbf{1}_{\{\theta \le 2r\}}, \qquad 0 \le \theta \le \pi.$$

In particular, if $r = \pi/2$ then $C(\theta) = 1 - \theta/\pi$ decays linearly throughout. Taylor expansions imply that the correlation function has fractal index $\alpha = 1$ for all $r \in (0, \pi/2)$, so that the corresponding Gaussian particles have non-smooth boundaries of Hausdorff dimension $\frac{5}{2}$.

4.3. Power kernel

Our third example is the power kernel, where the isotropic kernel k is defined as

$$k(\theta) = \left(\frac{\theta}{\pi}\right)^{-q} - 1, \qquad 0 < \theta \le \pi, \tag{8}$$

with power parameter $q \in (0, 1)$. The associated correlation function (2) takes the form

$$C(\theta) = \frac{2}{c_2} \int_0^\pi (\pi^q \lambda^{-q} - 1) \sin \lambda \int_{A(\lambda)} (\pi^q a(\theta, \lambda, \phi)^{-q} - 1) \, d\phi \, d\lambda, \tag{9}$$

where

$$t(\theta, \lambda, \phi) = \sin \theta \sin \lambda \cos \phi + \cos \theta \cos \lambda, \qquad a(\theta, \lambda, \phi) = \arccos t(\theta, \lambda, \phi),$$

and

$$A(\lambda) = \{\phi \in [0, \pi] : 0 < a(\theta, \lambda, \phi) \le \pi\}.$$

The normalising constant c_2 is here given by

$$c_2 = 2\pi \int_0^\pi (\pi^q \lambda^{-q} - 1)^2 \sin \lambda \, d\lambda = \frac{(q)_3}{6} \sum_{j=0}^\infty \frac{(-1)^j \pi^{2j+3}}{(2j+1)!} \frac{1}{(1-q+j)_3},$$

where $(a)_3 \equiv a(a+1)(a+2)$. This expression for c_2 is obtained by expanding $\sin \lambda$ in a Maclaurin series and then integrating the series termwise.

In our next result we show that the correlation function (9) has fractal index $\alpha = 2 - 2q$, so that the corresponding Gaussian particles have surfaces with Hausdorff dimension $2 + q$, as illustrated in Figure 1.

Theorem 2. *If $0 < q < 1$, the correlation function (9) satisfies*

$$\lim_{\theta \downarrow 0} \frac{C(0) - C(\theta)}{\theta^{2-2q}} = b_q, \tag{10}$$

where

$$b_q = \frac{2\pi^{2q}}{c_2} \int_0^\infty x^{1-q} \int_0^\pi (x^{-q} - (x^2 + 1 - 2x \cos \phi)^{-q/2}) \, d\phi \, dx \tag{11}$$

$$= \frac{\pi^{2q+1}}{c_2(1-q)^2} \frac{\Gamma(1 - (1/2)q)^2 \Gamma(q)}{\Gamma((1/2)q)^2 \Gamma(1-q)}. \tag{12}$$

In particular, the correlation function has fractal index $\alpha = 2 - 2q$.

We defer the proof of this result to Appendix A. The power kernel (8) has a negative exponent and, thus, is unbounded, which may lead to unbounded particle realisations. While values of $q < 0$ are feasible, they are of less interest, as the associated correlation functions have fractal index $\alpha = 2$, thereby generating smooth particles only.

5. Examples

Here, we demonstrate the flexibility of the Gaussian particle framework in simulation examples. First, we introduce a simulation algorithm. Then we simulate celestial bodies whose surface properties resemble those of the Earth, Moon, Mars, and Venus, as reported in the planetary physics literature. Furthermore, we study and simulate the planar particles that arise from the two-dimensional version of the particle model.

5.1. Simulation algorithm

To sample from the Gaussian particle model (1), we utilise the property that the underlying measure is independently scattered. Specifically, for every sequence (A_n) of disjoint Borel subsets of $\mathbb{S}^2$, the random variables $L(A_n)$, $n = 1, 2, \ldots$, are independent and $L(\cup A_n) = \sum L(A_n)$ almost surely. Let $(A_n)_{n=1}^N$ define an equal area partition of $\mathbb{S}^2$, so that $\lambda(A_n) = 4\pi/N$ for $n = 1, \ldots, N$. The random field X in (1) can then be decomposed into a sum of integrals over the disjoint sets A_n, in that

$$X(u) = \sum_{n=1}^{N} \int_{A_n} k(v, u) L(\mathrm{d}v), \qquad u \in \mathbb{S}^2.$$

For $n = 1, \ldots, N$ fix any point $v_n \in A_n$. We can then approximate the random field X by setting

$$x(u) = \sum_{n=1}^{N} k(v_n, u) L(A_n), \qquad u \in \mathbb{S}^2.$$

Let us denote the multivariate normal joint distribution of $L(A_1), \ldots, L(A_N)$ by F_N. To simulate a realisation y of the particle Y_c, we use the following algorithm.

Algorithm 1. 1. Set $M = M_1 M_2$, where M_1 and M_2 are positive integers, and construct a grid $u_1, \ldots, u_M$ on $\mathbb{S}^2$. Using spherical coordinates, let $u_m = (\theta_m, \phi_m)$ and put $\theta_m = i\pi/M_1$ and $\phi_m = 2\pi j/M_2$, where $m = iM_2 + j$ for $i = 0, 1, \ldots, M_1 - 1$ and $j = 1, \ldots, M_2$.

2. Apply the method of Leopardi (2006) to construct an equal area partition $A_1, \ldots, A_N$ of $\mathbb{S}^2$.

3. For $n = 1, \ldots, N$, let v_n have spherical coordinates equal to the mid range of the latitudes and longitudes within A_n, respectively.

4. For $n = 1, \ldots, N$, generate independent random variables L_n from F_N.

5. For $m = 1, \ldots, M$, set $x(u_m) = \max(c, \sum_{n=1}^{N} k(v_n, u_m) L_n)$.

6. Set y to be the triangulation of $\{(u_m, x(u_m)) : m = 1, \ldots, M\}$.

The equal area partitioning algorithm of Leopardi (2006) is a recursive zonal partitioning algorithm. That is, after appropriate polar cap areas have been removed, the sphere is divided into longitudinal zones, each of which is subsequently divided by latitude. By construction, the equal areal partition cells are continuity sets with respect to the intensity of the Gaussian measure, and in all our examples the kernel k is continuous almost everywhere.

This simulation procedure has been implemented in R (R Development Core Team (2009)), and code is available from the authors upon request. It can be considered an analogue of the moving average method (Oliver (1995), Cressie and Pavlicová (2002), Hansen and Thorarinsdottir (2013)) for simulating Gaussian random fields on Euclidean spaces. In principle, M and N can take any positive integer values. However, the usual tradeoff applies, in that the quality of the realisations increases with M_1, M_2, and N, at the expense of prolonged run times. For the realisations in Figures 1 and 5, we use $M_1 = 200$ and $M_2 = 400$, or $M = 8 \times 10^4$, and $N = 10^5$.

TABLE 1: Mean radius r_0, difference d_+ between maximal and mean radius, and difference d_- between minimal and mean radius, for Venus, dry Earth, Moon, and Mars, in kilometres.

	Body			
	Venus	Dry Earth	Moon	Mars
r_0	6051.8	6367.2	1737.1	3389.5
d_+	11.0	8.8	5.5	21.2
d_-	−3.0	−11.0	−12.0	−8.2

5.2. Celestial bodies

The geophysical literature has sought to characterise the surface roughness of the Earth and other celestial bodies in the solar system via the Hausdorff dimension of their topography (Mandelbrot (1982), Kucinskas *et al.* (1992)), with Turcotte (1987) arguing that the dimension is universal and equals about 2.5. Here, we provide simulated versions of the planets Earth, Venus, and Mars, and of the Moon, under the Gaussian particle model (1), with k being the power kernel (8). We set $q = \frac{1}{2}$, which provides the desired fractal dimension for a Gaussian particle surface, and choose the parameters

$$\mu = \frac{r_0}{c_1}, \qquad \sigma^2 = \frac{(d_+ - d_-)^2}{c_2}$$

of the Gaussian measure such that they correspond to reality. For this we use the information listed in Table 1, which was obtained from Price (1988), Jones and Stofan (2008), and online sources. The values concerning the Earth describe 'dry Earth'; to simulate 'wet Earth' we make a cutoff such that 29.2% of the area is land. Here, this corresponds to the Gaussian particle Y_c with truncation parameter $c = 6368.1$ kilometres. In principle, we also need to make a cutoff at $c = 0$ for 'dry Earth', but this is unnecessary in essentially all realizations. In our simulation algorithm, we use $M_1 = 200$, $M_2 = 400$, and $N = 10^6$ to obtain the celestial bodies in Figure 2. The corresponding radial functions along the equator are shown in Figure 3.
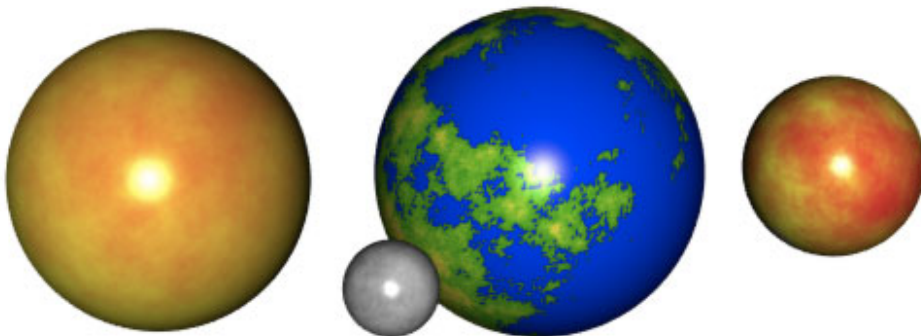

FIGURE 2: Simulations of Venus, the Moon, Earth, and Mars in true relative sizes.
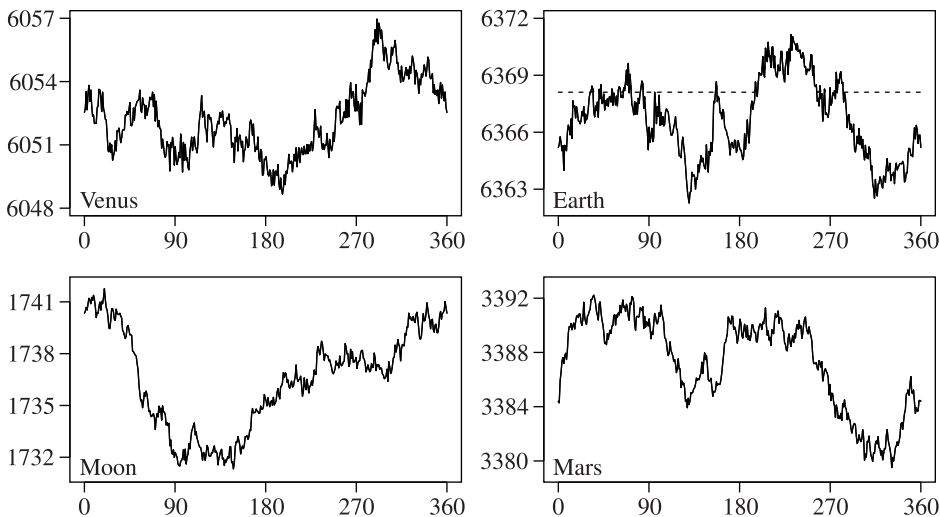
FIGURE 3: Radial function along the equator for the simulated bodies in Figure 2 in kilometres. Clockwise from upper left: Venus, Earth with ocean level indicated by a dashed horizontal line, Mars, and the Moon.

5.3. Planar particles

We now reduce the dimension and consider the planar Gaussian random particle

$$Y_c = \bigcup_{u \in \mathbb{S}^1} \{o + ru : 0 \le r \le \max(X(u), c)\} \subset \mathbb{R}^2.$$

Here $c > 0$, $o \in \mathbb{R}^2$ is an arbitrary centre, and the radial function $X(u)$ is modelled as

$$X(u) = \int_{\mathbb{S}^1} K(v, u) L(\mathrm{d}v), \qquad u \in \mathbb{S}^1,$$

with a suitable kernel function $K : \mathbb{S}^1 \times \mathbb{S}^1 \to \bar{\mathbb{R}}$ and a Gaussian measure L on the Borel subsets of the unit sphere $\mathbb{S}^1 = \{x \in \mathbb{R}^2 : \|x\| = 1\}$. We further construct planar gamma particles where L is a gamma measure on the Borel subsets of the unit sphere, $L(A) \sim \mathrm{Gamma}(\kappa \lambda(A), \tau)$ with shape $\kappa > 0$ and rate $\tau > 0$. Under this model, $\mu_X = \kappa c_1/\tau$ and $\sigma_X^2 = \kappa c_2/\tau^2$. The gamma measure is independently scattered and we can thus apply the same simulation method as for the Gaussian particles.

As previously, we assume that the kernel function K is isotropic, in that $K(v, u) = k(d(v, u))$ depends on the points $v, u \in \mathbb{S}^1$ through their angular or circular distance $d(v, u) \in [0, \pi]$, only. In Table 2 a list of the circular analogues of von Mises–Fisher, uniform, and power kernels is shown along with analytic expressions for the integrals

$$c_n = \int_{\mathbb{S}^1} k(d(v, u))^n \, \mathrm{d}v = 2 \int_0^\pi k(\eta)^n \, \mathrm{d}\eta,$$

where $n = 1, 2$, and the fractal index, α, of the associated correlation function, as defined in (3). The power kernel model has previously been studied by Wood ((1995) Example 3.3).

TABLE 2: Analytic form, parameter range, constants and associated fractal index for parametric families of isotropic kernels $k : [0, 2\pi) \to \bar{\mathbb{R}}$ on the circle $\mathbb{S}^1$.

	Kernel		
	von Mises–Fisher	Uniform	Power
Analytic form	$k(\theta) = e^{a \cos \theta}$	$k(\theta) = \mathbf{1}_{\{\theta \leq r\}}$	$k(\theta) = \left(\dfrac{\theta}{\pi}\right)^{-q} - 1$
Parameter	$a > 0$	$r \in \left(0, \dfrac{\pi}{2}\right]$	$q \in (-\frac{1}{2}, 0) \cup \left(0, \frac{1}{2}\right)$
c_1	$2\pi I_0(a)$	$2r$	$2\pi \dfrac{q}{1-q}$
c_2	$2\pi I_0(2a)$	$2r$	$4\pi \dfrac{q^2}{1 - 3q + 2q^2}$
Fractal index	2	1	$1 - 2q$

In an analogy to the respective result on $\mathbb{S}^2$, if $\max_{u \in \mathbb{S}^1} X(u) > c$, the boundary of the Gaussian particle Y_c has Hausdorff dimension $D = 2 - \alpha/2$ almost surely.

The general form of the associated correlation function is

$$C(\theta) = \frac{1}{c_2}\left(\int_{\pi-\theta}^{\pi} k(\phi)k(2\pi - \phi - \theta)\,d\phi + \int_0^{\pi-\theta} k(\phi)k(\theta + \phi)\,d\phi \right.$$
$$\left. + \int_0^{\theta} k(\phi)k(\theta - \phi)\,d\phi + \int_{\theta}^{\pi} k(\phi)k(\phi - \theta)\,d\phi\right), \qquad 0 \leq \theta \leq \pi.$$

For the von Mises–Fisher kernel with parameter $a > 0$, the correlation function admits the closed form

$$C(\theta) = \frac{I_0(a\sqrt{2(1 + \cos \theta)})}{I_0(2a)}, \qquad 0 \leq \theta \leq \pi,$$

where I_0 denotes the modified Bessel function of the first kind and of order 0, and for the uniform kernel with cutoff parameter $r \in (0, \pi/2]$, we have

$$C(\theta) = \left(1 - \frac{\theta}{2r}\right)\mathbf{1}_{\{\theta \leq 2r\}}, \qquad 0 \leq \theta \leq \pi.$$

For the power kernel with parameter $q \in (-\frac{1}{2}, 0) \cup (0, \frac{1}{2})$, tedious but straightforward computations result in a complex closed form expression, and a Taylor expansion about the origin yields the fractal index, $\alpha = 1 - 2q$, stated in Table 2.

Thus, the von Mises–Fisher and uniform kernels result in Gaussian particles with boundaries of Hausdorff dimension 1 and $\frac{3}{2}$, respectively. Under the power kernel, the Hausdorff dimension of the Gaussian particle surface is $\frac{3}{2} + q$. Simulated planar Gaussian and gamma particles with von Mises–Fisher, uniform, and power kernels are shown in Figure 4, with the parameter values varying by row, as listed in Table 3. The simulation algorithm of Section 5.1 continues to apply with natural adaptions, such as defining the simulation grid $u_m = 2\pi m/M$ for $m = 1, \ldots, M$, where we use $M = 5000$ and $N = 10^5$.

TABLE 3: Values of the parameter a for the von Mises–Fisher kernel, the parameter r for the uniform kernel, and the parameter q for the power kernel used to generate the planar particles in Figure 4.

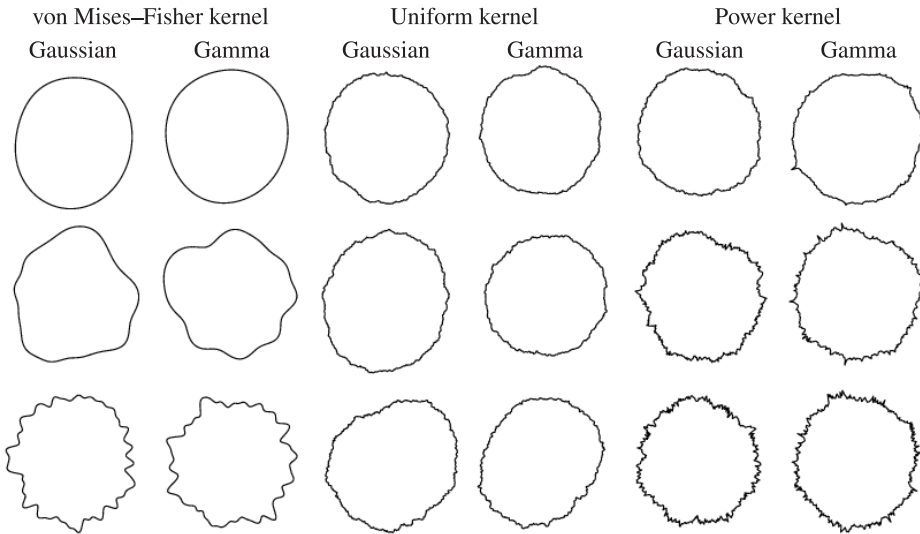| Row	a	r	q
1	3	1.5	0.05
2	30	1.0	0.25
3	300	0.5	0.45

FIGURE 4: Planar particles with mean $\mu_X = 25$ and variance $\sigma_X^2 = 10$. Columns 1 and 2 show particles generated using a von Mises–Fisher kernel, columns 3 and 4 particles using a uniform kernel, and columns 5 and 6 particles using a power kernel, with parameters varying by row as described in Table 3. The particles in columns 1, 3, and 5 are generated under a Gaussian measure, those in columns 2, 4, and 6 under a gamma measure.

6. Discussion

We have proposed a flexible framework for modelling and simulating star-shaped Gaussian random particles. The particles are represented by their radial function, which is generated by an isotropic kernel smoothing on the sphere. From a theoretical perspective, the construction is perfectly general, as every continuous isotropic correlation function on a sphere admits an isotropic convolution root (Ziegel (2014)). The Hausdorff dimension of the particle surface depends on the behaviour of the associated correlation function at the origin, as quantified by the fractal index. Under power kernels we obtain Gaussian particles with boundaries of any Hausdorff dimension between 2 and 3.

While a non-Gaussian theory remains elusive, we believe that similar results hold for gamma particles where $L(A) \sim \text{Gamma}(\kappa \lambda(A), \tau)$ in (1) with shape $\kappa > 0$ and rate $\tau > 0$. For instance, in Figures 1 and 5 we show Gaussian and gamma particles under the power kernel, respectively. The surface structures for the different bases resemble each other, even though the particles exhibit more pronounced spikes under the gamma basis, see also the planar particles
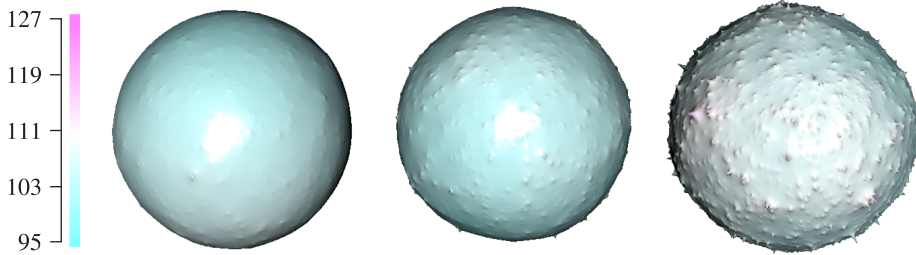
FIGURE 5: Gamma particles with mean $\mu_X = 100$ and variance $\sigma_X^2 = 10$, using a gamma measure in (1) and the power kernel (8) with $q = 0.05$ (left), $q = 0.25$ (middle) and $q = 0.5$ (right).

in Figure 4. Similar particle models may be generated using different types of Lévy bases L, such as Poisson or inverse Gaussian (Jónsdóttir *et al.* (2008)).

We have focused on three-dimensional particles, except for brief remarks on planar particles in the preceding section. However, the Gaussian particle approach generalises readily, to yield star-shaped random particles in $\mathbb{R}^d$ for any $d \geq 2$. The particles are represented by their radial function and associated with an isotropic random field on the sphere $\mathbb{S}^{d-1}$. In this setting, Estrade and Istas (2010) derive a recursion equation that yields closed form expressions for the isotropic correlation function on $\mathbb{S}^{d-1}$ that arises under a uniform kernel. Analogous to the terminology used in the Euclidean case (Gneiting (1999)), we refer to this correlation function as the 'spherical hat' function with cutoff parameter $r \in (0, \pi/2)$. Any spherical hat function has a linear behaviour at the origin, and, thus, has fractal index $\alpha = 1$. Estrade and Istas (2010) also show that scale mixtures of the spherical hat function provide correlation functions of any desired fractal index $\alpha \in (0, 1]$, similarly to the corresponding results of Hammersley and Nelder (1955) and Gneiting (1999) in the Euclidean case.

A far-reaching, natural extension of our approach uses nonisotropic kernels to allow for so-called multifractal particles, where the roughness properties and the Hausdorff dimension may vary locally on the particle surface. This fits the framework of Gagnon *et al.* (2006), who argue that the topography of the Earth is multifractal, and allows for multifractal simulations of three-dimensional celestial bodies, as opposed to extant work that applies to the topography of the 'Flat Earth'.

We have not discussed parameter estimation under our modelling approach, leaving this to future work. In a Bayesian setting, inference could be performed similarly to the methods developed by Wolpert and Ickstadt (1998), who use a construction akin to the random field model in (1) to represent the intensity measure of a spatial point process, and propose a simulated inference framework, where the model parameters, the underlying random field, and the point process are updated in turn, conditional on the current state of the other variables. Alternatively, Ziegel (2013) proposes a nonparametric inference framework based on series of Gegenbauer polynomials.

Appendix A. Proof of Theorem 2

We proceed in two parts, demonstrating first the asymptotic expansion (10) with the constant b_q in (11), and then establishing the equality of the expressions in (11) and (12), which confirms that b_q is strictly positive. The claim about the fractal index is then immediate from Theorem 1.

In what follows, if $A(\cdot)$ and $B(\cdot)$ are nonnegative functions on a common domain, we write

$$A \lesssim B$$

if there is a constant $C > 0$ such that $A \leq CB$ and C is independent of any parameters or arguments appearing in A and B when the latter are allowed to vary in their specified domains.

A.1. Asymptotic expansion (10)

Recall that

$$C(\theta) = \frac{2}{c_2} \int_0^\pi (\pi^q \lambda^{-q} - 1) \sin \lambda \int_{A(\lambda)} (\pi^q a(\theta, \lambda, \phi)^{-q} - 1) \, d\phi \, d\lambda,$$

where

$$t(\theta, \lambda, \phi) = \sin \theta \sin \lambda \cos \phi + \cos \theta \cos \lambda, \qquad a(\theta, \lambda, \phi) = \arccos t(\theta, \lambda, \phi),$$

and

$$A(\lambda) = \{\phi \in [0, \pi] \colon 0 < a(\theta, \lambda, \phi) \leq \pi\}.$$

Therefore,

$$\frac{c_2}{2} (C(0) - C(\theta)) = \int_0^\pi (\pi^q \lambda^{-q} - 1) \sin \lambda \left\{ \int_0^\pi (\pi^q \lambda^{-q} - 1) \, d\phi \right.$$
$$\left. - \int_{A(\lambda)} (\pi^q a(\theta, \lambda, \phi)^{-q} - 1) \, d\phi \right\} d\lambda.$$

Since $A(\lambda) = [0, \pi]$ for $\lambda \in (0, \pi - \theta]$ and $A(\lambda) \subset [0, \pi]$ for $\lambda \in (\pi - \theta, \pi)$, we decompose the integral on the right-hand side as $P_{1q}(\theta) + P_{2q}(\theta)$, where $P_{1q}(\theta)$ and $P_{2q}(\theta)$ correspond to the integral with respect to λ over $(0, \pi - \theta)$ and $(\pi - \theta, \pi)$, respectively. The first mean value theorem for integration implies that there exists a $t \in (\pi - \theta, \pi)$ such that

$$P_{2q}(\theta) = \theta(\pi^q t^{-q} - 1) \sin t \left\{ \int_0^\pi (\pi^q t^{-q} - 1) \, d\phi - \int_{A(t)} (\pi^q a(\theta, t, \phi)^{-q} - 1) \, d\phi \right\}.$$

Hence, $P_{2q}(\theta)$ decays at least as fast as $\mathcal{O}(\theta^2)$ as $\theta \downarrow 0$.

As regards the first term, substituting $\lambda = \theta x$ yields

$$P_{1q}(\theta) = \theta^{2-2q} \pi^{2q} \int_0^{(\pi-\theta)/\theta} \frac{\sin(\theta x)}{\theta} (x^{-q} - \pi^{-q} \theta^q) \int_0^\pi (x^{-q} - a(\theta, \theta x, \phi)^{-q} \theta^q) \, d\phi \, dx.$$

In order to prove the asymptotic behaviour (10) it now suffices to show that

$$\lim_{\theta \downarrow 0} I(\theta) = \frac{c_2}{2\pi^{2q}} b_q = \int_0^\infty x^{1-q} f(0, x) \, dx, \tag{13}$$

where

$$I(\theta) = \int_0^{(\pi-\theta)/\theta} \frac{\sin(\theta x)}{\theta} (x^{-q} - \pi^{-q} \theta^q) f(\theta, x) \, dx$$

for $\theta > 0$, with

$$f(\theta, x) = \int_0^\pi (x^{-q} - a(\theta, \theta x, \phi)^{-q} \theta^q) \, d\phi$$

for $x > 0$ and $\theta \geq 0$. As we aim to find the limit $\lim_{\theta \downarrow 0} I(\theta)$, we may assume that $\theta \in (0, \theta_0)$ for some $0 < \theta_0 \ll 1$, and that $\lambda \in [0, \pi - \theta]$.

Lemma 1. *We have $t(\theta, \lambda, \phi) \le \cos(\theta - \lambda)$ and*

$$a(\theta, \lambda, \phi)^{-q} \le |\theta - \lambda|^{-q}.$$

Proof. We write

$$t(\theta, \lambda, \phi) = \sin\theta \sin\lambda \cos\phi + \cos\theta \cos\lambda = \cos(\theta - \lambda) + \sin\theta \sin\lambda(\cos\phi - 1).$$

Since $\cos\phi - 1 \in [-2, 0]$ and the inverse cosine function is monotonically decreasing, the claims follow.

Lemma 2. *Define $f(0, x) = \lim_{\theta \downarrow 0} f(\theta, x)$. Then the limit exists and equals*

$$f(0, x) = \int_0^\pi (x^{-q} - (x^2 - 2x\cos\phi + 1)^{-q/2})\, \mathrm{d}\phi$$

for $x \notin \{0, 1\}$.

Proof. For $x \notin \{0, 1\}$ fixed, the integrand in the definition of $f(\theta, x)$ is bounded in ϕ. The claim follows immediately from the limit

$$\lim_{\theta \downarrow 0} = \frac{a(\theta, \theta x, \phi)}{\theta} = (x^2 - 2x\cos\phi + 1)^{1/2}$$

along with Lebesgue's dominated convergence theorem. Indeed, noting that

$$\frac{\arccos(t)}{\theta} = \frac{\arccos(1 - y^2)}{y} \frac{y}{\theta}\Bigg|_{y=(1-t)^{1/2}}$$

for $t \in (0, 1)$, we find that

$$\lim_{\theta \downarrow 0} \frac{a(\theta, \theta x, \phi)}{\theta} = \frac{\mathrm{d}}{\mathrm{d}y}\arccos(1 - y^2)\Bigg|_{y=0} \lim_{\theta \downarrow 0}\left(\frac{1 - \cos\theta \cos\theta x}{\theta^2} - \frac{\sin\theta \sin\theta x}{\theta^2}\cos\phi\right)^{1/2}$$
$$= (x^2 - 2x\cos\phi + 1)^{1/2}.$$

Lemma 3. *We have*

$$|f(\theta, x)| \le \pi(x^{-q} + |x - 1|^{-q})$$

for $x \in [0, (\pi - \theta)/\theta]$.

Proof. We find from Lemma 1 that

$$a(\theta, \theta x, \phi)^{-q}\theta^q \le |x - 1|^{-q},$$

and the claim follows.

For later purposes we need to find the Taylor expansion of $a(\theta, \lambda, \phi)^{-q}$ around $\theta = 0$,

$$a(\theta, \lambda, \phi)^{-q} = a(0, \lambda, \phi)^{-q} + \frac{\mathrm{d}}{\mathrm{d}\theta}a(\theta, \lambda, \phi)^{-q}\Bigg|_{\theta=0}\theta + R(\theta, \lambda, \phi),$$

where R denotes the error term.

Lemma 4. *We have*

$$a(\theta, y, \phi)^{-q} = y^{-q} + \frac{q \cos \phi}{y^{q+1}} \theta + R(\theta, y, \phi),$$

where the error term satisfies

$$|R(\theta, y, \phi)| \lesssim \theta^2 \left(\frac{1}{|y - \theta|^{q+2}} + \frac{1}{|y - \theta|^{q+1} \sin(y - \theta)} \right)$$

for $y \in [2\theta, \pi - \theta]$.

Proof. From $t(0, y, \phi) = \cos y$, the zeroth-order term is immediately seen to be y^{-q}. For the first-order term, we compute

$$\frac{\mathrm{d}}{\mathrm{d}\theta} a(\theta, y, \phi) = -\frac{1}{\sqrt{1 - t^2}} (\cos \theta \sin y \cos \phi - \sin \theta \cos y),$$

so

$$\left. \frac{\mathrm{d}}{\mathrm{d}\theta} a(\theta, y, \phi) \right|_{\theta=0} = -\cos \phi.$$

Hence,

$$\left. \frac{\mathrm{d}}{\mathrm{d}\theta} a(\theta, y, \phi)^{-q} \right|_{\theta=0} = -\frac{q}{a(0, y, \phi)^{q+1}} \left. \frac{\mathrm{d}}{\mathrm{d}\theta} a(\theta, y, \phi) \right|_{\theta=0} = \frac{q \cos \phi}{y^{q+1}}.$$

To estimate R, we present it in Lagrange form,

$$R(\theta, y, \phi) = \frac{1}{2} \left. \frac{\mathrm{d}^2}{\mathrm{d}\theta^2} a(\theta, y, \phi)^{-q} \right|_{\theta=\hat{\theta}} \theta^2,$$

for some $\hat{\theta} \in [0, \theta]$. Then, we have

$$\frac{\mathrm{d}^2}{\mathrm{d}\theta^2} a(\theta, y, \phi)^{-q} = \frac{\mathrm{d}}{\mathrm{d}\theta} \left(-\frac{q}{a(\theta, y, \phi)^{q+1}} \frac{\mathrm{d}}{\mathrm{d}\theta} a(\theta, y, \phi) \right)$$

$$= \frac{q(q + 1)}{a(\theta, y, \phi)^{q+2}} \left(\frac{\mathrm{d}}{\mathrm{d}\theta} a(\theta, y, \phi) \right)^2 - \frac{q}{a(\theta, y, \phi)^{q+1}} \frac{\mathrm{d}^2}{\mathrm{d}\theta^2} a(\theta, y, \phi)$$

$$= A(\theta, y, \phi) + B(\theta, y, \phi).$$

Let us now estimate $A(\theta, y, \phi)$ from above for $y \in [2\theta, \pi - \theta]$. From

$$\frac{1}{\sqrt{1 - t^2}} \leq \frac{1}{\sqrt{1 - \cos^2(y - \theta)}} = \frac{1}{\sin(y - \theta)}$$

we obtain

$$\left| \frac{\mathrm{d}}{\mathrm{d}\theta} a(\theta, y, \phi) \right| \leq \frac{\sin y + \sin \theta}{\sin(y - \theta)}.$$

By monotonicity, we have $\sin \theta \leq \sin(y - \theta)$ and $\sin y \leq 2 \sin(y - \theta)$. Hence, in view of Lemma 1, we find that

$$|A(\theta, y, \phi)| \lesssim |y - \theta|^{-q-2}$$

for $y \in [2\theta, \pi - \theta]$.

To estimate $B(\theta, y, \phi)$ in the same range, we compute

$$\frac{\mathrm{d}^2}{\mathrm{d}\theta^2} a(\theta, y, \phi) = C(\theta, y, \phi) + D(\theta, y, \phi),$$

where

$$C(\theta, y, \phi) = \frac{\mathrm{d}}{\mathrm{d}\theta}\left(-\frac{1}{\sqrt{1-t^2}}\right)(\cos\theta \sin y \cos\phi - \sin\theta \cos y)$$

$$= -\frac{t}{(1-t^2)^{3/2}}(\cos\theta \sin y \cos\phi - \sin\theta \cos y)^2$$

and

$$D(\theta, y, \phi) = -\frac{1}{\sqrt{1-t^2}}\frac{\mathrm{d}}{\mathrm{d}\theta}(\cos\theta \sin y \cos\phi - \sin\theta \cos y)$$

$$= \frac{1}{\sqrt{1-t^2}}(\sin\theta \sin y \cos\phi + \cos\theta \cos y).$$

We have

$$\frac{|t|}{(1-t^2)^{3/2}} \le \frac{|\cos(y-\theta)|}{\sin^3(y-\theta)} \le \frac{1}{\sin^3(y-\theta)}$$

for $y \in [2\theta, \pi - \theta]$. Hence,

$$|C(\theta, y, \phi)| \le \frac{(\sin y + \sin\theta)^2}{\sin^3(y-\theta)} \lesssim \frac{1}{\sin(y-\theta)}.$$

Similarly, $|D(\theta, y, \phi)| \lesssim 1/(\sin(y-\theta))$. Hence,

$$|B(\theta, y, \phi)| \lesssim \frac{1}{|y-\theta|^{q+1}\sin(y-\theta)}$$

for $y \in [2\theta, \pi - \theta]$.

Finally, for $\hat\theta \in [0, \theta]$,

$$|A(\hat\theta, y, \phi)| \lesssim \frac{1}{(y-\hat\theta)^{q+2}} \le \frac{1}{|y-\theta|^{q+2}},$$

and, similarly,

$$|B(\hat\theta, y, \phi)| \lesssim \frac{1}{(y-\hat\theta)^{q+1}\sin(y-\hat\theta)} \lesssim \frac{1}{|y-\theta|^{q+1}\sin(y-\theta)}.$$

Combining the estimates for A and B, the proof of the lemma is complete.

In what follows, we need the classical estimate

$$0 \le \frac{\sin\theta x}{\theta} \le x, \tag{14}$$

for $x \ge 0$ and $\theta > 0$.

Lemma 5. *We have*

$$\frac{\sin\theta x}{\theta}|f(\theta, x)| \lesssim (x-1)^{-1-q}$$

for $x \in [2, (\pi - \theta)/\theta]$.

Proof. From Lemma 4 and $\int_0^\pi \cos\phi\, d\phi = 0$, we find

$$f(\theta, x) = \theta^{q+2} \int_0^\pi R(\hat\theta, \theta x, \phi)\, d\phi.$$

Using Lemma 4 and (14), we obtain

$$\frac{\sin\theta x}{\theta}|f(\theta, x)| \lesssim \frac{\sin\theta x}{\theta}(x-1)^{-2-q} + \frac{\sin\theta x}{\sin\theta(x-1)}(x-1)^{-1-q} \lesssim (x-1)^{-1-q}.$$

Lemma 6. *We have that $x^{1-q} f(0, x)$ is Lebesgue integrable and*

$$\lim_{\theta\downarrow 0} I(\theta) = \int_0^\infty x^{1-q} f(0, x)\, dx.$$

Proof. From (14), Lemma 3, and Lemma 5, we find that

$$\left|\frac{\sin(\theta x)}{\theta}(x^{-q} - \pi^{-q}\theta^q) f(\theta, x)\right| \lesssim \begin{cases} x^{1-2q} + |x-1|^{-q}, & x \in [0, 2], \\ (x-1)^{-1-2q} + (x-1)^{-1-q}, & x \in [2, \infty), \end{cases}$$

uniformly in $\theta \in (0, \theta_0]$, where $0 < \theta_0 \ll 1$. Since the latter function is Lebesgue integrable, the claims follow from Lebesgue's dominated convergence theorem along with Lemma 2.

This completes the proof of (13) and, therefore, of the asymptotic relationship (10) with the constant b_q in (11).

A.2. Equality of the expressions in (11) and (12)

We now show that the constant b_q is strictly positive. Specifically, we demonstrate the equality of the expressions in (11) and (12) for $q \in (0, 1)$. Toward this end, we first prove that

$$b_q = \frac{\pi^{2q+1}\Gamma(1 - (1/2)q)}{c_2\Gamma((1/2)q)} \int_0^\infty t^{q-1}\big(1 - e^{-t}{}_1F_1(1 - \tfrac{1}{2}q; 1; t)\big)\frac{dt}{t}, \qquad (15)$$

where with $(x)_0 = 1$ and $(x)_n = x(x+1)\cdots(x+n-1)$ for $n = 1, 2, \ldots$, the classical confluent hypergeometric function (Digital Library of Mathematical Functions ((2011) Chapter 13)) can be written as

$$_1F_1(a; b; t) = \sum_{k=0}^\infty \frac{(a)_k}{(b)_k}\frac{t^k}{k!}.$$

We establish this representation as follows. With a keen eye on the inner integral in (11), we note that for $x > 0$ and $\phi \in (0, \pi)$,

$$x^{-q} = (x^2)^{-q/2} = \frac{1}{\Gamma((1/2)q)} \int_0^\infty e^{-tx^2} t^{q/2}\frac{dt}{t},$$

and

$$(1 + x^2 - 2x\cos\phi)^{-q/2} = \frac{1}{\Gamma((1/2)q)} \int_0^\infty e^{-t(1+x^2-2x\cos\phi)} t^{q/2}\frac{dt}{t}.$$

Substituting these equations into (11), and interchanging the order of the integration with respect to ϕ and t, we obtain

$$b_q = \frac{2\pi^{2q}}{c_2\Gamma((1/2)q)} \int_0^\infty x^{1-q} \int_0^\infty t^{q/2}e^{-tx^2} \int_0^\pi (1 - e^{-t(1-2x\cos\phi)})\, d\phi \frac{dt}{t}\, dx. \qquad (16)$$

By well-known equations,

$$\int_0^\pi e^{t\cos\phi}\,d\phi = \pi I_0(t) = \pi\,_0F_1\big(1;\tfrac{1}{4}t^2\big),$$

where I_0 denotes the modified Bessel function of the first kind of order 0, and $_0F_1$ is a special case of the generalised hypergeometric series (Digital Library of Mathematical Functions ((2011) Equations 10.32.1 and 10.39.9)). Therefore,

$$\int_0^\pi (1 - e^{-t(1-2x\cos\phi)})\,d\phi = \pi(1 - e^{-t}\,_0F_1(1; t^2x^2)).$$

Substituting this result into (16), and interchanging the order of the integration, we obtain

$$b_q = \frac{2\pi^{2q+1}}{c_2\Gamma((1/2)q)}\int_0^\infty t^{q/2}\int_0^\infty x^{1-q}e^{-tx^2}(1 - e^{-t}\,_0F_1(1; t^2x^2))\,dx\,\frac{dt}{t}. \qquad (17)$$

With the substitution $x = u^{1/2}$, we obtain

$$\int_0^\infty x^{1-q}e^{-tx^2}\,dx = \frac{1}{2}t^{(1/2)q-1}\Gamma\big(1 - \tfrac{1}{2}q\big).$$

We apply next a well-known equation for the Laplace transforms of generalised hypergeometric series (Digital Library of Mathematical Functions ((2011) Equation 16.5.3)) to obtain, with the substitution $x = t^{-1/2}u^{1/2}$,

$$\int_0^\infty x^{1-q}e^{-tx^2}\,_0F_1(1; t^2x^2)\,dx = \frac{1}{2}t^{(1/2)q-1}\Gamma\big(1 - \tfrac{1}{2}q\big)\,_1F_1\big(1 - \tfrac{1}{2}q; 1; t\big).$$

Consequently, by (17), we have established the representation (15).

Finally, we apply the Kummer equation for the $_1F_1$ function (Digital Library of Mathematical Functions ((2011) Equation 13.2.39)) to show that

$$1 - e^{-t}\,_1F_1\big(1 - \tfrac{1}{2}q; 1; t\big) = \tfrac{1}{2}qt\,_2F_2\big(\tfrac{1}{2}q + 1, 1; 2, 2; -t\big).$$

Thus, by the representation (15),

$$b_q = \frac{\pi^{2q+1}q}{2c_2}\frac{\Gamma(1 - (1/2)q)}{\Gamma((1/2)q)}\int_0^\infty t^q\,_2F_2\big(\tfrac{1}{2}q + 1, 1; 2, 2; -t\big)\frac{dt}{t},$$

and this integral is a well-known Mellin transform; see Digital Library of Mathematical Functions ((2011) Equation 16.5.1), where the integral is given in inverse Mellin transform format (Digital Library of Mathematical Functions ((2011) Section 1.14(iv))). The proof of the equality of the expressions in (11) and (12) is now complete.

Acknowledgements

References

ADLER, R. J. (2010). *The Geometry of Random Fields*. Society for Industrial and Applied Mathematics, Philadelphia, PA.

CRESSIE, N. AND PAVLICOVÁ, M. (2002). Calibrated spatial moving average simulations. *Statist. Modelling* **2,** 267–279.

DIGITAL LIBRARY OF MATHEMATICAL FUNCTIONS (2011). Release 2011-07-01. Available at http://dlmf.nist.gov.

DO CARMO, M. P. (1976). *Differential Geometry of Curves and Surfaces*. Prentice-Hall, Englewood Cliffs, NJ.

ESTRADE, A. AND ISTAS, J. (2010). Ball throwing on spheres. *Bernoulli* **16,** 953–970.

FALCONER, K. (1990). *Fractal Geometry: Mathematical Foundations and Applications*. John Wiley, Chichester.

FISHER, N. I., LEWIS, T. AND EMBLETON, B. J. J. (1987). *Statistical Analysis of Spherical Data*. Cambridge University Press.

GAGNON, J.-S., LOVEJOY, S. AND SCHERTZER, D. (2006). Multifractal earth topography. *Nonlinear Process. Geophys.* **13,** 541–570.

GANGOLLI, R. (1967). Positive definite kernels on homogeneous spaces and certain stochastic processes related to Lévy's Brownian motion of several parameters. *Ann. Inst. H. Poincaré B* **3,** 121–226.

GNEITING, T. (1999). Radial positive definite functions generated by Euclid's hat. *J. Multivariate Anal.* **69,** 88–119.

GRENANDER, U. AND MILLER, M. I. (1994). Representations of knowledge in complex systems. *J. R. Statist. Soc. B* **56,** 549–603.

HALL, P. AND ROY, R. (1994). On the relationship between fractal dimension and fractal index for stationary stochastic processes. *Ann. Appl. Prob.* **4,** 241–253.

HAMMERSLEY, J. M. AND NELDER, J. A. (1955). Sampling from an isotropic Gaussian process. *Proc. Camb. Phil. Soc.* **51,** 652–662.

HANSEN, L. V. AND THORARINSDOTTIR, T. L. (2013). A note on moving average models for Gaussian random fields. *Statist. Prob. Lett.* **83,** 850–855.

HAUSDORFF, F. (1918). Dimension und äußeres Maß. *Math. Ann.* **79,** 157–179.

HOBOLTH, A. (2003). The spherical deformation model. *Biostatistics* **4,** 583–595.

HOBOLTH, A., KENT, J. T. AND DRYDEN, I. L. (2002). On the relation between edge and vertex modelling in shape analysis. *Scand. J. Statist.* **29,** 355–374.

HOBOLTH, A., PEDERSEN, J. AND JENSEN, E. B. V. (2003). A continuous parametric shape model. *Ann. Inst. Statist. Math.* **55,** 227–242.

JONES, R. H. (1963). Stochastic processes on a sphere. *Ann. Math. Statist.* **34,** 213–218.

JONES, T. AND STOFAN, E. (2008). *Planetology: Unlocking the Secrets of the Solar System*. National Geographic, Washington, D.C..

JÓNSDÓTTIR, K. Y., SCHMIEGEL, J. AND JENSEN, E. B. V. (2008). Lévy-based growth models. *Bernoulli* **14,** 62–90.

KENT, J. T., DRYDEN, I. L. AND ANDERSON, C. R. (2000). Using circulant symmetry to model featureless objects. *Biometrika* **87,** 527–544.

KUCINSKAS, A. B. *et al.* (1992). Fractal analysis of Venus topography in Tinatin Planitia and Ovda Regio. *J. Geophys. Res. Planets* **97,** 13635–13641.

LEOPARDI, P. (2006). A partition of the unit sphere into regions of equal area and small diameter. *Electron. Trans. Numer. Anal.* **25,** 309–327.

MANDELBROT, B. B. (1982). *The Fractal Geometry of Nature*. W. H. Freeman, San Francisco, CA.

MILLER, M. I. *et al.* (1994). Membranes, mitochondria and amoebae: shape models. *J. Appl. Statist.* **21,** 141–163.

MUINONEN, K. *et al.* (1996). Light scattering by Gaussian random particles: ray optics approximation. *J. Quant. Spectrosc. Radiat. Transfer* **55,** 577–601.

MUÑOZ, O. *et al.* (2007). Scattering matrix of large Saharan dust particles: experiments and computations. *J. Geophys. Res. Atmospheres* **112,** D13215.

OLIVER, D. S. (1995). Moving averages for Gaussian simulation in two and three dimensions. *Math. Geology* **27,** 939–960.

ORFORD, J. D. AND WHALLEY, W. B. (1983). The use of the fractal dimension to quantify the morphology of irregular-shaped particles. *Sedimentology* **30,** 655–668.

PRICE, F. W. (1988). *The Moon Observer's Handbook*. Cambridge University Press.

R DEVELOPMENT CORE TEAM (2009). *R: A Language and Environment for Statistical Computing*. R Foundation for Statistical Computing, Vienna, Austria. Available at http://www.r-project,org

STOYAN, D. AND STOYAN, H. (1994). *Fractals, Random Shapes and Point Fields*. John Wiley, Chichester.

TOVCHIGRECHKO, A. AND VAKSER, I. A. (2001). How common is the funnel-like energy landscape in protein-protein interactions? *Protein Sci.* **10,** 1572–1583.

TURCOTTE, D. L. (1987). A fractal interpretation of topography and geoid spectra on the Earth, Moon, Venus, and Mars. *J. Geophys. Res. Solid Earth* **92,** E597–E601.

WICKSELL, S. D. (1925). The corpuscle problem. A mathematical study of a biometric problem. *Biometrika* **17,** 84–99.

WOLPERT, R. L. AND ICKSTADT, K. (1998). Poisson/gamma random field models for spatial statistics. *Biometrika* **85,** 251–267.

WOOD, A. T. A. (1995). When is a truncated covariance function on the line a covariance function on the circle? *Statist. Prob. Lett.* **24,** 157–164.

XUE, Y. AND XIAO, Y. (2011). Fractal and smoothness properties of space–time Gaussian models. *Front. Math. China* **6,** 1217–1248.

ZIEGEL, J. (2013). Stereological modelling of random particles. *Commun. Statist. Theory Meth.* **42,** 1428–1442.

ZIEGEL, J. (2014). Convolution roots and differentiability of isotropic positive definite functions on spheres. *Proc. Amer. Math. Soc.* **142,** 2063–2077.